

Is there a link between very high strain and metastable phases in semiconductors: cases of Si and GaAs?

P Puech¹, F Demangeot¹, Paulo Sergio Pizani², V Domnich³ and Y Gogotsi³

¹ Laboratoire de Physique des Solides, Université Paul Sabatier-IRSAMC-CNRS, 31062 Toulouse Cédex, France

² Departamento de Física, Universidade Federal de São Carlos, CP 369, 13560-970 São Carlos, SP, Brazil

³ Department of Materials Engineering, Drexel University, LeBow Building, 3141 Chestnut Street, Philadelphia, PA 19104, USA

Received 31 July 2003

Published 22 December 2003

Online at stacks.iop.org/JPhysCM/16/S39 (DOI: 10.1088/0953-8984/16/2/005)

Abstract

Silicon and gallium arsenide indentations have been investigated by using Raman spectroscopy. This perfect tool permits the study of the strain field within and around the indentation with 3D-micrometric resolution. By mapping both indented materials, we show that the strain varies strongly in GaAs and is constant in Si within indentations. With the selected orientation of GaAs, the two observed phonons provide a way to determine the local symmetry of the strain in all the area of the fingerprint. In Si, the quite constant value within the indentation, always reported in the literature with low laser power, seems to be correlated with the metastable phases created. To provide evidence for this fact, we have selected samples which favour metastable phases over amorphous, allowing the study of the correlation of the Raman peaks associated with metastable crystalline Si phases (Si-XII) and associated with diamond Si-I. The frequency shift plot of the 355 cm⁻¹ band as a function of the Si-I Raman band frequency at 522 cm⁻¹ exhibits a negative slope. The strains in both phases have an opposite sign. This accurate observation provides an insight into the origin of the surprising high strain in silicon.

1. Introduction

Micro- and nano-indentation is now a widespread technique for hardness testing measurements. Due to the small size of the contact area between material surface and indenter, high pressures can be reached. The properties of Si after indentation have been intensively studied during the last decade [1–4]. Gallium arsenide is not so well documented [5–7].

Raman spectroscopy is a perfect tool for studying the strain field. The spot light has an area of about 1 μm^2 , with a probe depth limited by the optical properties of the semiconductor studied. Consequently, local information is easily obtained without any treatment. Lower

resolutions than x-ray are not damageable; the large deformation in the range of 1% or 0.1% is easily covered by both techniques.

Molecular dynamics calculations have shown that an extensive and compressive zone can be found around indentation in Si_3N_4 while within the indentation, residual compressive strain and amorphous phases are found [8]. In the case of silicon, it is very hard to find diamond extensive phases. No clear report on this point can be found in the literature. In the case of silicon, the laser annealing of amorphous phases gives signatures of hexagonal phases located in the range 509–519 cm^{-1} [4, 9]. As a consequence, within the indentation, a careful analysis is needed to investigate the presence of tensile strain. To our knowledge, no clear evidence is available for high tensile strain within silicon indentations. In all indentations tested in our laboratory, no large tensile strain has been found in the fingerprint.

On the one hand measurement of the stress magnitude in the crystalline Si-I phase (cd, cubic diamond) in the micro-indentation region has been addressed experimentally by micro-Raman spectroscopy in several papers [1–4]. These Raman analyses are generally based on the literature concerning the Raman signature in silicon under stress [10]. Frequency shifts of the Si-I Raman band varying from 522 cm^{-1} , far from the indentation centre, to 527 cm^{-1} when probing the 1 N load indentation site are reported by Lucazeau *et al* [3]. Localized regions near cracks in the impression have been found to be highly strained (shift of the Si-I Raman band as high as 536 cm^{-1}). Stress relaxation around a 1 N load micro-indentation has also been reported by one of us [4], by careful Raman mapping, pointing out the laser heating effect. Such high strain is usually observed in superlattices where the creation of dislocations or gliding planes is not possible.

On the other hand, phase transformations in Si have not received a lot of attention. If the appearance of amorphous silicon in the impression centre has been reported in all the previously cited works, the experimental analysis of metastable crystalline phases of Si are rare and mainly performed by Domnich and Gogotsi [1], Kailer *et al* [2] and Demangeot *et al* [11]. The hexagonal diamond phase (Si-IV or hd), body-centred cubic phase (Si-III or bc8) and its rhombohedral distortion (Si-XII or r8) have been reported by Raman signatures at various wavelengths between 200 and 500 cm^{-1} , based on both experimental and previous theoretical results. These authors proposed a scheme of the phases transformations that occurs during hardness indentations and post-treatment in silicon [1, 2].

The mechanical properties of III–V polar semiconductors, like GaAs, have not been intensively investigated; only a few previous reports deal with micro-indented and microscratched GaAs [11, 13]. No new phase has been created within the indentation as expected by physical arguments. In a previous work, we have explore the strain field along a line and shown that the stress tensor is purely biaxial [12]. The complex profile, starting at the centre at compressive strain value changes quickly to tensile between the centre and the edge to become compressive at the edge of the fingerprint.

In this paper, we report observations within silicon and gallium arsenide indentations. Firstly, the AFM images of the fingerprints under study are shown. Then, we discuss the frequency shifts through Raman mapping. The comparison of the two materials suggests a possible correlation between high strain value and phases existence. Several nano-indentations are used to answer this question.

2. Samples, theory and experiments

2.1. Samples

The silicon nano-indentation test was performed using a Berkovich pyramid as described in a previous work [11]. Using silicon substrate, we can create within the indentation a new

phase. By varying the loading and unloading speeds, an amorphous phase or crystalline metastable phases are preferentially obtained. For silicon, nano-indentation is favourable to phase creation. The loading rates ranged from 0.3 to 1 mN s⁻¹, and the maximum loads used were in the range 30–100 mN. With these conditions, metastable phases are created and no amorphous status is expected. The same rates were used for loading and unloading. The gallium arsenide micro-indentation was performed using a Vickers Indentor with 1 N load. No particular rates are used as no phase creation is expected.

2.2. Theory

Strain induces frequency shift. This effect is calculated by the diagonalization of the modulation of the dynamical matrix. Eigenvalues $d\omega$ correspond to the phonon frequency shift and eigenvectors \mathbf{e}_a to the polarization of the associated phonon. In a biaxial strained layer, singlet (S) and doublet (D) components refer to the strain and correspond to the Z axis (S component) and direction in the plane of the layer (D component) [15]. In the case of silicon, three optical phonons are degenerated in the centre of the Brillouin zone. Strain splits this degeneracy into three components. The conversion factor is obtained by working out the calculation if the symmetry is well known, or experimentally in other cases. For silicon indentation, it has been shown experimentally that the conversion factor $d\omega = -670\varepsilon_{\parallel}$ for a (001) surface is quite good [4]. For GaAs, the electro-optic effect leads to two sets of equations: one for TO and one for LO. With the (111) sample crystallographic orientation, both optical phonons can be observed in the spectra. In a previous work, we have shown that the strain field is locally biaxial (the off-diagonal component of the strain tensor is not accessible using Raman spectroscopy with polar material). With this hypothesis for TO, the conversion factor to obtain strain is $d\omega_{\text{TO}} = -670\varepsilon_{\parallel}$ [11].

2.3. Experiments

Raman spectra were recorded in backscattering geometry on the (001) surface of an undoped Si wafer using a Renishaw spectrometer ($\lambda = 514$ nm) for mapping and a Dilor XY spectrometer for wavelength studies (in the range 647–488 nm). For undoped GaAs oriented along (111), mapping has been realised using a Renishaw spectrometer. The spatial resolution in these experiments is suited to a value of around $0.6 \mu\text{m}^2$, thanks to the use of high numerical aperture microscope objectives $100\times$. We took care to keep the laser power in the sample in the low range (<0.5 mW) in order to prevent any major heating effects [4]. Si and GaAs indentation images presented in figures 1 and 2 have been recorded by atomic force microscopy with a Park Scientific Instruments (model AutoProbe CP) in contact mode. We used SiN AFM tips with a conical shape and with a radius at the end of the tip of 5–10 nm, giving the estimated spatial resolution for this image.

3. First observations

3.1. AFM-Si

A surface topography measurement of the impression region is presented in figure 1. This 2D AFM image gives a view of a 100 mN load nano-indentation area from above. The typical size of the impression lies in the 2–3 μm range with a clear triangular trace related to the triangular shape of the diamond indenter. Dark contrast indicates a lower topography area while light contrast gives higher surface points. The image contrast (which is to some extent related to the interaction between the tip and the material surface) exhibits slight differences in comparison

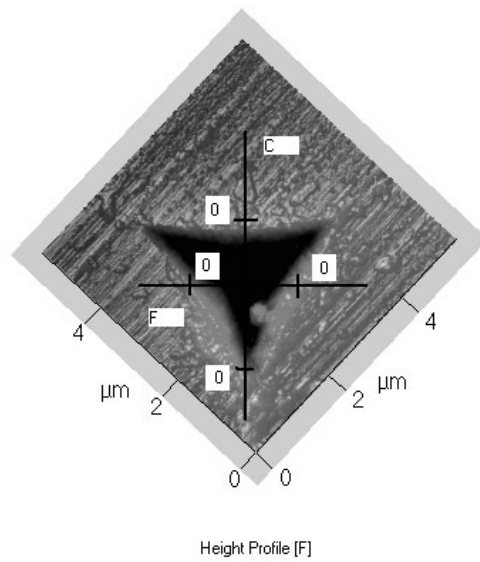


Figure 1. AFM image of (001)-Si nano-indentations.

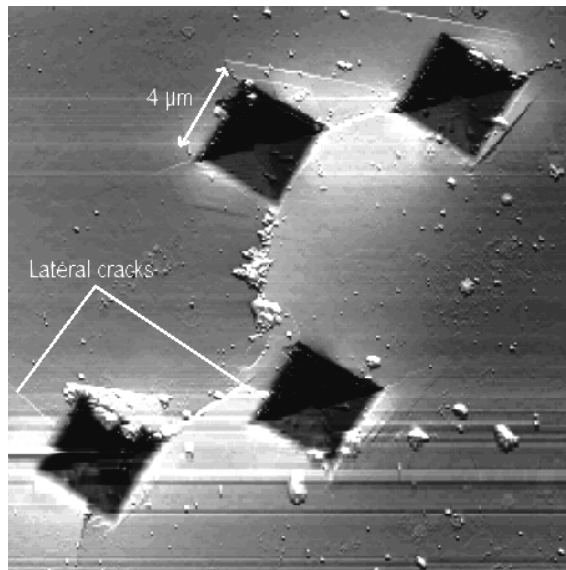


Figure 2. AFM image of (111)-GaAs indentations. Some lateral cracks, orthogonal to the borders, are indicated. The size of the fingerprint is $4 \times 4 \mu\text{m}$.

with the contrast observed far from the trace region, leading to the assumption that the nature of the extruded material is not crystalline Si, but rather crystalline metastable phase Si.

3.2. AFM-GaAs

As for Si, the AFM image of the GaAs impression region is shown in figure 2. We can see several lines in the figure. The lines around the indentation along $\langle 110 \rangle$ generic direction correspond to sudden height changes and have C_{3v} symmetry, as the (111) face of the substrate.

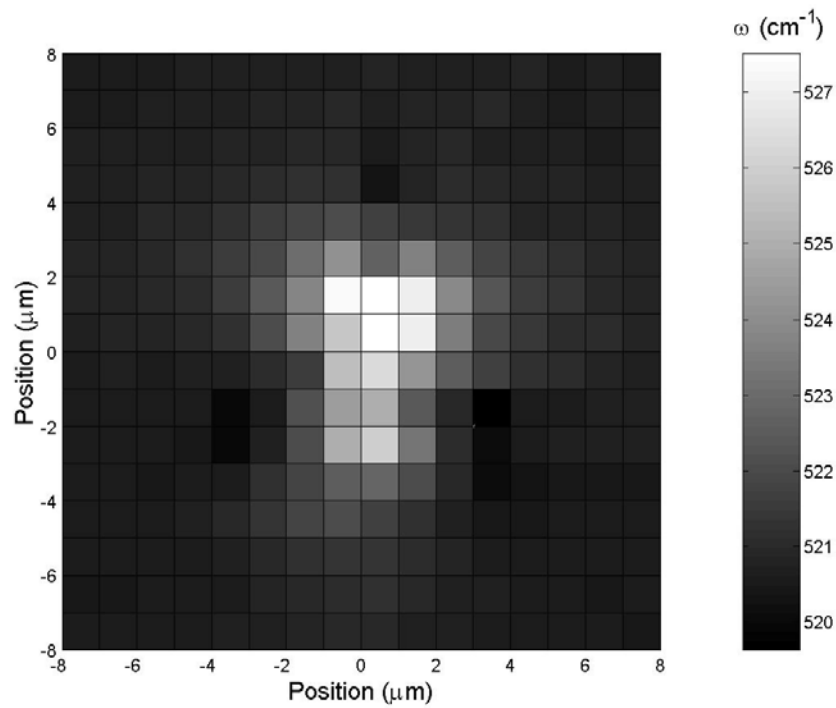


Figure 3. Raman image of Si nano-indentation: optical phonon.

More interesting is the lateral cracks in the centre of the edge, as indicated in figure 2. These defects are not related to the symmetry of the material but are related to the symmetry of the indenter. We suspect that these relaxation defects are due to the impossible relaxation of a tensile and extensive strain through gliding planes and dislocations.

3.3. Raman-Si

We show in figure 3 the strain field determined by Raman spectroscopy. The Berkovich indenter shape leads to highly anisotropic strain. In this particular case, we observe near the edges of the indentation a small extensive area, corresponding to a -1 cm^{-1} shift to the lower frequencies. Within the indentation, only compressive strain is found. When cracks are present with large load, the frequency shifts to the upper values.

3.4. Raman GaAs

We present in figure 4 a mapping within the indentation. As TO shifts twice to LO, it is four times more intense than LO and perfectly homothetic to LO, we report the TO data in figure 4 and the plot in figure 5 of LO versus TO frequency. The biaxial hypothesis is confirmed in all areas of the fingerprint. Let us turn to TO. We first observe that TO shifts both sides of the reference value. In the centre, the observed value is positive, corresponding to the compressive case. Around this centre, a highly tensile value is found. This could be related to transversal cracks indicated by the AFM image in figure 2. Within the indentation, near the border, a compressive value surrounded the negative one. The highest shift ($+2.5 \text{ cm}^{-1}$) corresponds to an in-plane deformation of -0.5% . The lowest shift (-2.5 cm^{-1}) corresponds to an in-plane

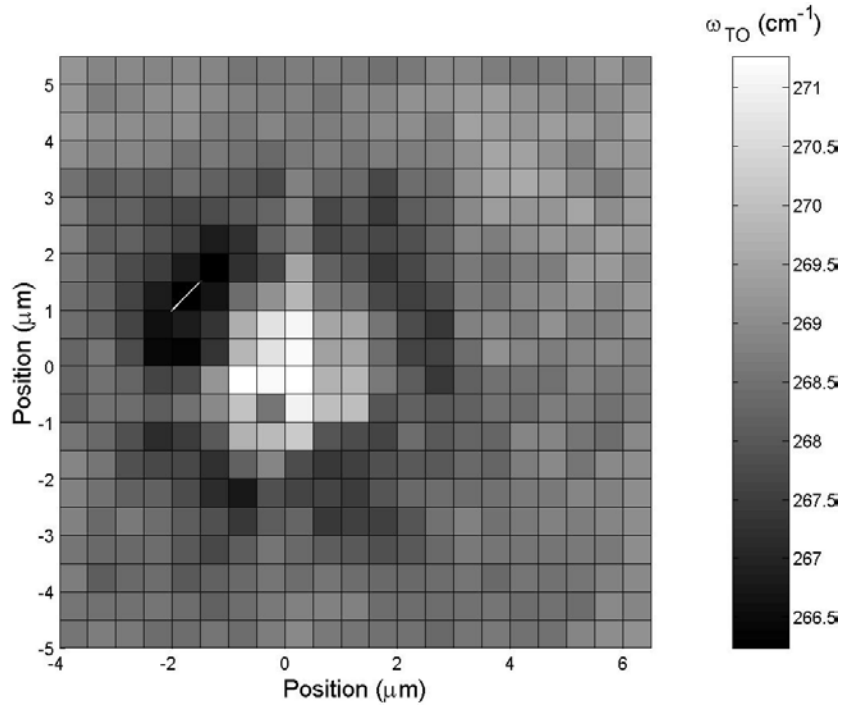


Figure 4. Raman image of (111)-GaAs micro-indentation: TO frequency.

deformation of +0.5%. Within the indentation, the variation of the in-plane deformation is equal to 1%, which is close to the value obtained with silicon. No new phase has been detected within the indentations.

3.5. Comparison

Under uniaxial stress experiments, the observed stress limit corresponds to 1.2 GPa along (111) for GaAs [14]. In our case, 1.2 GPa corresponds to a frequency shift of 4.7 cm^{-1} . These values are in the range of GaAs observed values. In the case of silicon, the accommodation is better and no limit is indicated in Raman stress measurements [15]. The biaxial conversion factor for both LO-Si along (001) and TO-GaAs along (111) is $\Delta\omega = -670\varepsilon_{\parallel}$. So, we can compare directly frequency shifts.

For silicon, the lowest value is slightly negative, less than -1 cm^{-1} , but outside the indentation. Within the indentation, the highest value found is around $7\text{--}8 \text{ cm}^{-1}$. This value is in fact quite constant in all areas of the fingerprint.

For gallium arsenide, within the indentation, the lowest value observed (-2.5 cm^{-1}) is in the opposite sign than the highest value ($+2.5 \text{ cm}^{-1}$) but has the same absolute value. The same behaviour has been found in other indentations. Gogotsi *et al* [5] have reported a similar shift; nevertheless, this strain value associated to this shift is lower than the residual strain in Si.

To find any origin of the lack of tensile strain within the Si fingerprint, we will test the hypothesis in which phases could play a key role.

4. Keeping strain

In order to probe various strained indentations, we have realized three sets of nano-indentations with 30, 70 and 100 mN load. Strain in amorphous phases is impossible to probe; the location

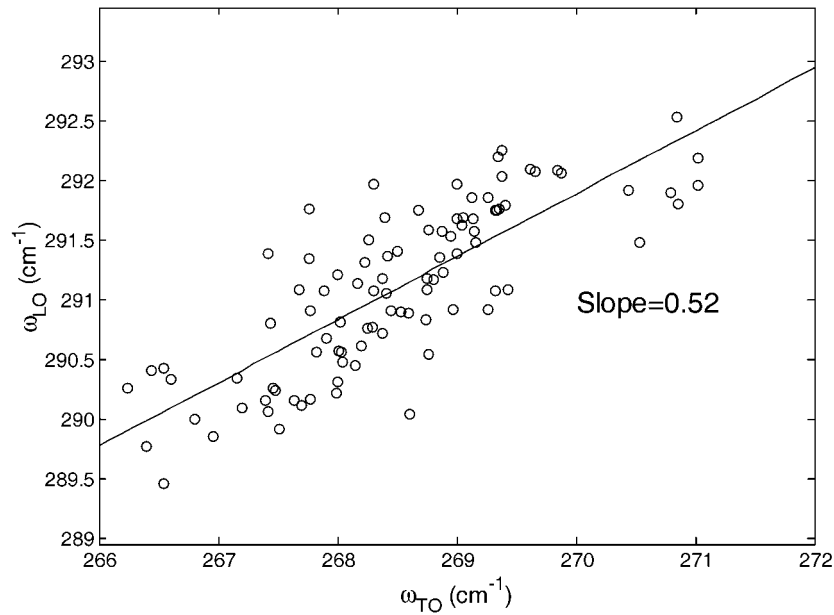


Figure 5. LO frequency versus TO frequency within the indentation. The slope 0.5 corresponds to the biaxial case (while 2 corresponds to the uniaxial case).

of the optic band is correlated to the distortion of the tetrahedra and a small shift of this band cannot be separated between disorder and strain contribution. Consequently, we have used nano-indentation with no amorphous phases but large metastable phases. In this way, we access the various strains in both diamond and Si-XII phases. Because this analysis needs the curve fitting of a lot of spectra, with the higher spectral resolution, it was almost impossible to complete this study for all the peaks. So we decided to limit this approach to the 355 cm^{-1} mode. The frequency range of the Si-XII phase varies from 354.5 to 353.5 cm^{-1} . Some typical spectra recorded within indentations are reported in figure 6. Several indentations with each load have been realised, giving the opportunity of making a statistical analysis. The sizes of the indentation are in the micrometre range. The spot size integrates over a gradient of strain. Nevertheless, by fitting with a symmetric Lorentzian, the mean value is obtained. When looking at figure 6, we can notice that spectrum (a) presents an asymmetry to the lower frequency for the diamond mode (522 cm^{-1}) while the 355 cm^{-1} peaks presents an asymmetry to the upper frequency. This observation is systematic and valid for all the exciting wavelengths (blue to red). Raman measurements under hydrostatic pressure have been reported by Olinjyk *et al* [16] and show that both peaks shift to the upper frequencies (positive Grüneisen parameter) when pressure is applied. If we plot the frequency of the Si-XII phase at 355 cm^{-1} versus the frequency of the diamond Si at 522 cm^{-1} , we can observe in figure 7 an anticorrelation between them. The experimental slope corresponds to a value of -0.3 . From Grüneisen parameters, the ratio of Si-XII phonon frequency shifts versus Si-I frequency equals $+0.3$. The strain can be decomposed in an anisotropic part and in an isotropic part. The isotropic part always gives the absolute sign of the shift. So, comparing the Grüneisen parameter is an acceptable approximation to determine a mean strain value inside phases. Consequently, we can conclude that the opposite strain in sign inside both phases is present. If we consider that the two phases are linking and the sudden change in the lattice parameter kept as a constant, a relaxation of Si XII, which reduces the strain

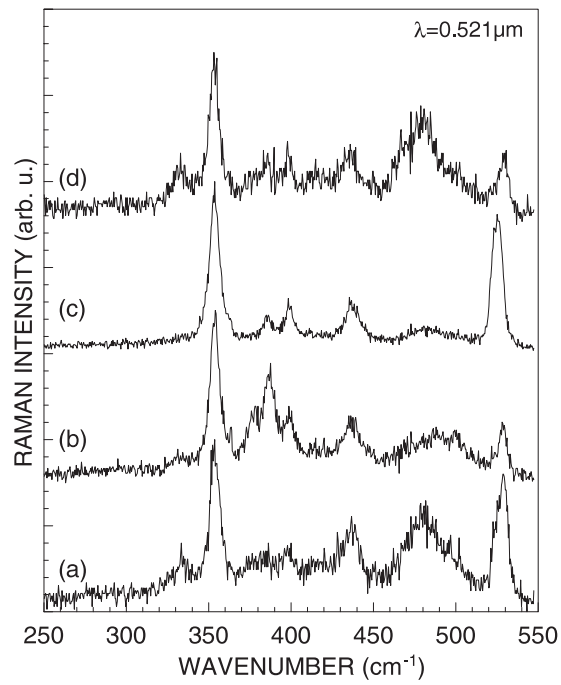


Figure 6. Typical Raman spectra in Si nano-indentations.

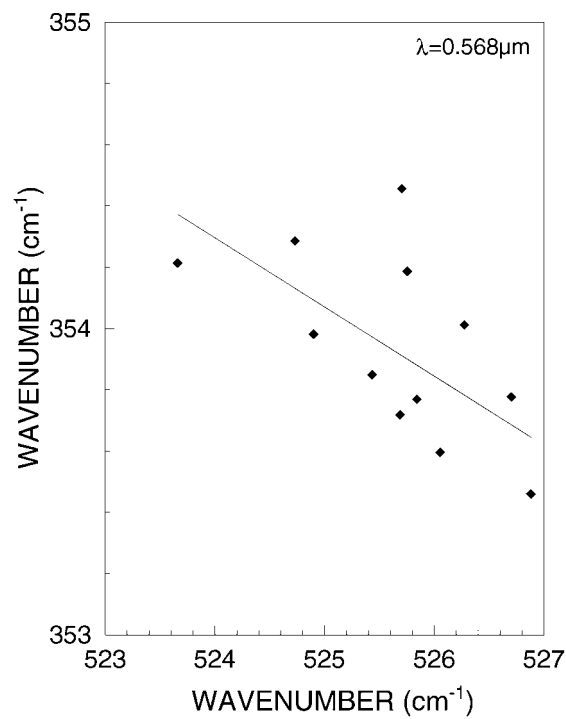


Figure 7. Phonon frequencies indicate the strain field in the metastable phases versus the strain field in diamond silicon.

energy of this phase, will increase the strain energy of the other phase Si I. As a consequence, the high strain value observed in Si-I could be directly correlated to the presence of other phases.

5. Conclusion

In gallium arsenide, no new phase has been observed. The Raman mapping shows that the phonon frequency shifts for both optical phonons within the indentation varies from a positive to a negative value. The in-plane deformation deduced from these phonon frequency shifts varies from 0.5% to -0.5% . The local biaxial behaviour is confirmed within all the area of the indentation. These results are in contrast with silicon indentation where a very high constant strain around 1% is obtained. This high strain has been tentatively correlated to the presence of other phases (amorphous and crystalline metastable). In the case of nano-indentation, using several loads, we have shown for the first time that the strain in the metastable phases has the opposite sign to that in the surrounding diamond Si. Our measurements suggest that the strain value inside the indentation is strongly correlated to phases. A local equilibrium between strain energy inside both phases could be at the origin of this experimental observation.

References

- [1] Domnich V and Gogotsi Y 2002 *Rev. Adv. Mater. Sci.* **3** 1
- [2] Kailer A, Nickel K G and Gogotsi Y G 1999 *J. Raman Spectrosc.* **30** 939–46
- [3] Lucazeau G and Abello L 1997 *J. Mater. Res.* **12** 2262
- [4] Puech P, Pinel S, Jasinevicius R G and Pizani P S 2000 *J. Appl. Phys.* **88** 4582
- [5] Gogotsi Y G, Domnich V, Dub S N, Kailer A and Nickel K G 2000 *J. Mater. Res.* **15** 871
- [6] Domnich V and Gogotsi Y 2001 *Frontiers of High-Pressure Research II: Application of High Pressure to Low Dimensional Novel Electronic Materials* ed H D Hochheimer, B Kuchta, P K Dorhout and J L Yarger (Dordrecht: Kluwer–Academic) pp 29, 302
- [7] Puech P, Demangeot F, Pizani P S, Wey S and Fontaine C 2003 *J. Mater. Res.* **18** 1474
- [8] Walsh P, Kalia R K, Nakano A, Vashista P and Saini S 2000 *Appl. Phys. Lett.* **77** 4332
- [9] Bandet J, Despax B and Caumont M 2002 *J. Phys. D: Appl. Phys.* **34** 1
- [10] Anastassakis E and Liarokapis E 1987 *J. Appl. Phys.* **62** 3346
- [11] Demangeot F, Puech P, Paillard V, Domnich V and Gogotsi Y G 2002 *Solid State Phenom.* **82–84** 777–82
- [12] Puech P, Landa G, Carles R and Fontaine C 1997 *J. Appl. Phys.* **82** 4493
- [13] Pizani P S, Lanciotti F Jr, Jasinevicius R G, Duduch J G and Porto A J V 2000 *J. Appl. Phys.* **87** 1280
- [14] Wickboldt P, Anastassakis E, Sauer R and Cardona M 1987 *Phys. Rev. B* **35** 1362
- [15] Cerdeira C, Buchenauer C J, Pollak F H and Cardona M 1972 *Phys. Rev. B* **5** 580
- [16] Olinjyk H and Jephcoat A P 1999 *Phys. Status Solidi b* **211** 413